Tuning carrier mobility without spin transport degrading in copper-phthalocyanine

S. W. Jiang, P. Wang, B. B. Chen, Y. Zhou, H. F. Ding' , and D. Wu'

Citation: Appl. Phys. Lett. **107**, 042407 (2015); doi: 10.1063/1.4927676
View online: http://dx.doi.org/10.1063/1.4927676
View Table of Contents: http://aip.scitation.org/toc/apl/107/4
Published by the American Institute of Physics

Tuning carrier mobility without spin transport degrading in copper-phthalocyanine

S. W. Jiang,[1] P. Wang,[1] B. B. Chen,[1] Y. Zhou,[1] H. F. Ding,[1,2,a)] and D. Wu[1,2,a)]
[1]*National Laboratory of Solid State Microstructures and Department of Physics, Nanjing University, 22 Hankou Road, Nanjing 210093, People's Republic of China*
[2]*Collaborative Innovation Center of Advanced Microstructures, Nanjing University, 22 Hankou Road, Nanjing 210093, People's Republic of China*

(Received 31 March 2015; accepted 19 July 2015; published online 29 July 2015)

We demonstrate more than one order of magnitude of carrier mobility tuning for the copper-phthalocyanine (CuPc) without spin transport degrading in organic spin valve devices. Depending on the preparation conditions, organic spin valves with the CuPc film mobility of 5.78×10^{-3} and 1.11×10^{-4} cm^2/V s are obtained for polycrystalline and amorphous CuPc, respectively. Strikingly, the spin diffusion lengths are almost the same regardless of their mobilities that are ~50 times different, which is in sharp contrast with previous prediction. These findings directly support that the spin relaxation in CuPc is dominated by the spin-orbit coupling. © *2015 AIP Publishing LLC*.
[http://dx.doi.org/10.1063/1.4927676]

The possibility of the use of spin in organic semiconductor devices such as organic light-emitting diodes (OLEDs) and memristor to enhance the device performance has received growing attention since a relatively large magnetoresistance (MR) of ~40% was obtained in a vertical organic spin valve (OSV).[1–3] Understanding their spin transport properties is of pivotal importance to develop high performance devices. There is, however, an ongoing debate regarding the mechanisms of the spin relaxation in organic semiconductors. The hyperfine interaction (HFI) and the spin-orbit coupling (SOC) are the both possible origins of the spin relaxation and they have been extensively studied, both experimentally[4,5] and theoretically.[6,7] A longer spin diffusion length λ_s and a weaker effect on the magneto-electroluminescence effect were observed in a polymer after replacing hydrogen atoms with deuterium atoms, leading to a conclusion that the HFI is the cause of the spin relaxation mechanism.[4] In contrast, the magneto-electroluminescence effect on the deuterated aluminium tris(8-hydroxyquinoline) (Alq_3) did not show difference from the protonated Alq_3, implying that the HFI does not play a dominant role in spin flipping.[8] However, Nguyen *et al*. observed substantial isotope dependence on Alq_3 in the measurements of magneto-electroluminescence effect, conductivity-detected magnetic resonance in diodes, and MR in OSVs, supporting the HFI induced spin relaxation mechanism.[9] Although the SOC is a primary source of the spin relaxation in inorganic semiconductors, the direct experimental evidence for this on organic materials has been lacking. The conventional approach to study the role of the SOC in organic materials is to choose a molecule with heavy ions, expecting a strong SOC strength.[10] Our recent work, however, showed that the heavy ion does not exhibit strong SOC strength in the spin-polarized polaron transport due to the quenching of the orbital moment by the ligand field.[11] The role of the SOC in the spin relaxation needs to be studied in a new approach.

The carrier mobility μ in organic semiconductors is a crucial parameter to determine the performance of organic devices. It is also believed that μ can significantly influence the spin transport.[12,13] For example, an order of millimeter spin diffusion length was predicted for a high-mobility single-crystalline rubrene according to an experiment on a low-mobility amorphous rubrene.[14] In fact, it is still unclear how μ changes λ_s experimentally. Moreover, tuning mobility is a good approach to discriminate different spin relaxation mechanisms. For HFI, the spin is relaxed due to a precession around a total effective HFI field and an applied field while it localizes on a molecule, meaning that the dwell time on molecule or μ can influence λ_s.[6,15] For SOC, the spin is flipped by the SOC as it hops from one molecule to another, meaning that the hopping distance determines λ_s and thereby μ does not have much impact on λ_s.[7] Therefore, to both understanding the spin relaxation mechanisms and control the device performance, the study of the spin transport in materials with tunable mobility is essential.

Copper-phthalocyanine (CuPc) is a typical *p*-type semiconductor. CuPc and other phthalocyanine derivatives have been widely used in electro-optic devices, field effect transistor, and photoelectric devices. The mobility of CuPc can be controlled from ~10^{-5} to ~10^{-2} cm^2/V s by simply changing the growth conditions,[16] suggesting that it is a good candidate to study the correlation of the mobility and the spin relaxation mechanisms in the same material. In this work, we use CuPc as a spacer to fabricate $La_{0.66}Sr_{0.34}MnO_3$ (LSMO)/CuPc/Co OSVs, for which CuPc films are grown in different conditions. The film grown at high temperature and low growth rate is polycrystalline structure with mobility of 5.78×10^{-3} cm^2/V s. In comparison, the film grown at low temperature and high rate is amorphous with mobility of 1.11×10^{-4} cm^2/V s. It is found that the OSVs with high mobility CuPc show lower MR ratio than OSVs with low mobility CuPc, probably due to the stronger spin scattering at rough Co/CuPc interfaces. Although the mobilities of these CuPc films are significantly different, the spin diffusion lengths are observed

a)Electronic addresses: hfding@nju.edu.cn and dwu@nju.edu.cn

to be almost the same. This result directly suggests that the crystallinity and mobility do not have impact on spin diffusion length and the SOC is the dominant spin relaxation source in CuPc.

The fabrication process of OSVs has been described in detail elsewhere.[11] The LSMO film was ultrasonically cleaned in acetone, ethanol, and deionized water in sequence and reused multiple times to fabricate OSVs without observing any apparent degradation. Purified CuPc was thermally evaporated under a pressure of $<2\times10^{-7}$ Torr. A calibrated quartz crystal thickness monitor is located next to the sample to measure the film thickness. Two different preparation conditions for CuPc films were performed: evaporation at a rate of 0.1 Å/s with substrate temperature ~100 °C and then annealed it at ~200 °C for 1 h (CuPc-1); evaporation at a rate of 20 Å/s with substrate temperature is ~−100 °C (CuPc-2). Co electrode was deposited by a so-called indirect deposition method to reduce the Co/CuPc interfacial inter-diffusion.[17] The device has a cross-bar geometry with an active area about 0.2 mm × 0.2 mm. Approximately 200 nm thick CuPc films were prepared under different growth conditions on LSMO for X-ray diffraction (XRD) and reflection high energy electron diffraction (RHEED) measurements. The surface morphology of the CuPc films was characterized by atomic force microscopy (AFM). After the fabrication of OSVs, the samples were immediately transferred into a vacuum chamber of a close-cycle system to carry out the magneto-transport measurements. The samples were measured in a four-point configuration with an applied field in the sample plane.

Figure 1(a) presents the XRD patterns of the CuPc films deposited under two different conditions. The film of CuPc-1 exhibits a single sharp peak at 2θ of 6.9°, indicating a polycrystalline structure with the interlayer distance of 12.9 Å. The interlayer distance corresponds to the diffraction from the (200) lattice plane of the α-phase CuPc separated by approximately the inter-stacking distances, implying that the trace of the herringbone pattern is parallel to the substrate, as shown in the inset of Fig. 1(a). These results are consistent with the previous reports.[16,18] The average grain size is estimated to be ~57 nm from the width of the diffraction peak using the Scherrer formula. In contrast, the XRD pattern of the CuPc-2 film shows no visible diffraction peaks, indicating an amorphous structure. The difference of these two types of films can also be seen from the surface morphology and RHEED patterns, as shown in Figs. 1(b)–1(e). The CuPc-1 film is composed of large rectangular grains and the average grain size is ~60 nm, in agreement with XRD results. The surface of the CuPc-1 film is much rougher than that of CuPc-2, manifested by the average roughness of 3.2 nm and 1.9 nm for CuPc-1 film and CuPc-2 film, respectively. Streak spots are observed for the CuPc-1 film and no diffraction pattern is observed for CuPc-2 film in RHEED patterns, confirming that the CuPc-1 film is polycrystalline and the CuPc-2 film is amorphous.[19] The crystallization of CuPc-1 is due to the fact that the low deposition rate and the high growth temperature allow molecules to have enough time and energy to reach the thermodynamical position. The crystallized CuPc-1 should have much less structural

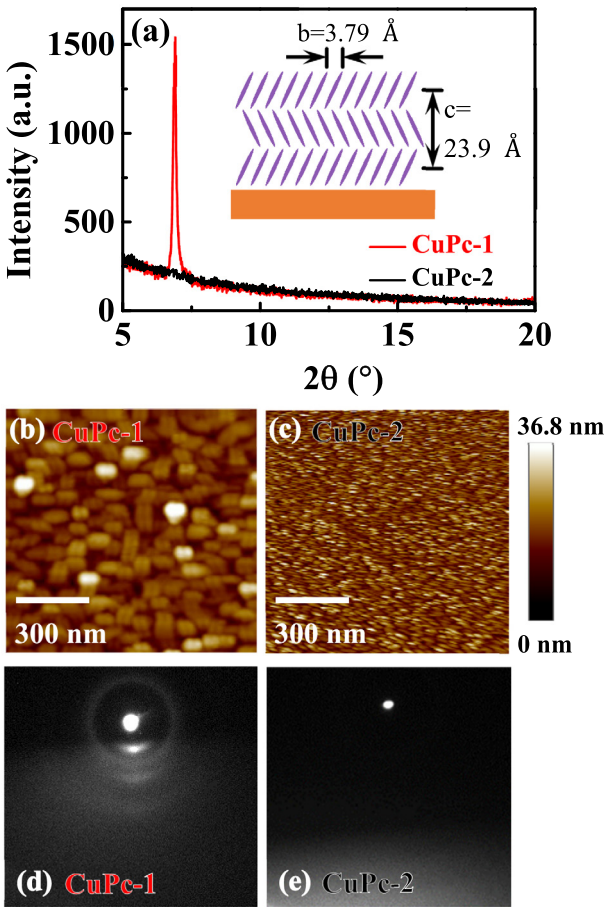

FIG. 1. (a) XRD patterns of CuPc-1 and CuPc-2 films grown on LSMO. The inset shows the schematic crystal structure of the α-phase of CuPc in *a*-axis projection. AFM images of (b) CuPc-1 and (c) CuPc-2 films grown on LSMO. RHEED patterns of (d) CuPc-1 and (e) CuPc-2 films grown on LSMO.

disorders than the amorphous CuPc-2, which means less traps and higher mobility.

In order to understand the charge transport mechanism of two types of CuPc films, the electrical transport measurements were performed on the OSV devices. The current-voltage (*J-V*) characteristics of LSMO (50 nm)/CuPc (110 nm)/Co (20 nm) OSVs with CuPc-1 film (device 1) and CuPc-2 film (device 2) as spacer, respectively, measured at temperature $T=10$ K are shown in Fig. 2. Clearly, the current of device 1 is nearly two orders of magnitude larger than that of device 2. The work functions of LSMO and Co are ~4.9 (Ref. 20) and ~5.0 eV,[21] respectively, which are comparable with an ionization potential of CuPc (4.8 eV).[22] Therefore, a hole-only device is expected and the carrier injection barrier should be very small at the LSMO/CuPc and Co/CuPc interfaces.[23,24] The *J-V* curves can be discriminated by two distinct regimes. In the low voltage regime ($V<0.1$ V), J depends linearly on V. The carrier is mainly generated by the thermally excitation. In the high voltage regime ($V>0.3$ V), J scales quadratically with V. Considering that traps may exist in CuPc films, such behavior is attributed to trap-filled space charge limited current (TFSCLC) behavior.[25,26] The TFSCLC is given by $J=9/8\varepsilon_0\varepsilon_r\mu V^2/d^3$, where ε_0 is the permittivity of vacuum, $\varepsilon_r=3.6$ is the relative permittivity of CuPc,[27] and d

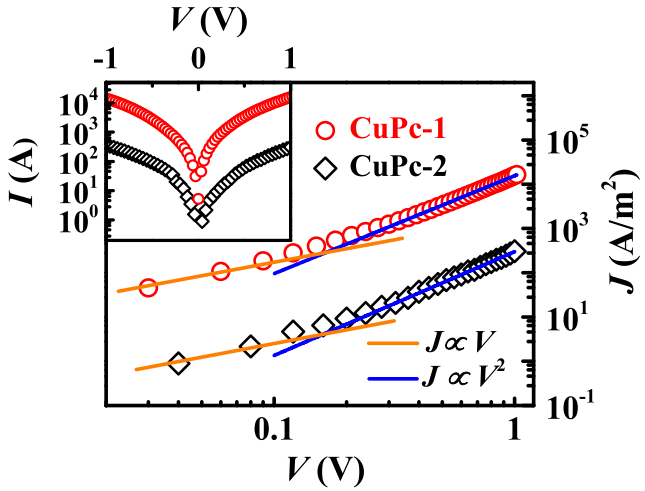

FIG. 2. *J-V* curves of CuPc-1 and CuPc-2 OSV devices with the CuPc thickness of 110 nm, measured at $T = 10$ K. The solid lines are the linear and quadratic fitting results. Inset: full range *I–V* curves on a semilog coordinate.

is the film thickness. From the fitting by TFSCLC model, the mobilities of the CuPc-1 film and CuPc-2 film are estimated to be 5.78×10^{-3} and 1.11×10^{-4} cm^2/V s, respectively. We note that ε_r may be different due to different crystallinity. ε_r is small and generally between 2 and 5 in organic materials,[28] suggesting that the difference of two types of CuPc films should be small. When the difference of ε_r is considered, the mobility of the CuPc-1film is still much larger than that of the CuPc-2 film. This result is in agreement with the previous result that the CuPc carrier mobility can be significantly enhanced by the improved crystallinity.[16] Moreover, owing to the π-π stacking direction of CuPc film in film plane, the observed mobility, current perpendicular to plane, of the crystallized CuPc is smaller than that of a similar CuPc film measured in field effect transistor geometry, current in plane.[29]

Figures 3(a) and 3(b) show the typical MR curves of devices 1 and 2 measured at $V = -0.1$ V. The OSVs clearly exhibit an inverse or negative spin valve effect, similar to LSMO/Alq_3/Co OSVs.[1,17] The MR ratio gradually decreases with increasing temperature for both devices, as shown in the insets of Figs. 3(a) and 3(b). At room temperature, an MR ratio of 0.84% and 0.50% for devices 1 and 2, respectively, is still observed. The temperature dependence of MR ratio is generally attributed to the increase of spin relaxation rate in organic semiconductors[1,30] and the decay of the spin polarization of LSMO with increasing temperature.[31,32] As

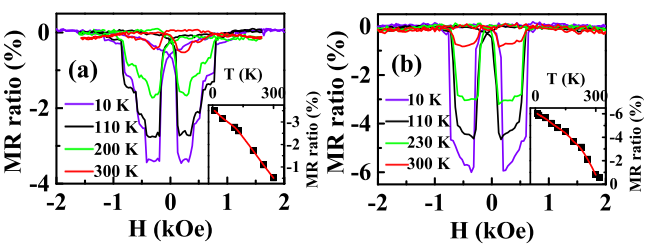

FIG. 3. MR loops of OSV devices based on (a) CuPc-1 and (b) CuPc-2 film with thickness of 110 nm, measured at different temperatures with a bias voltage of −0.1 V. The insets show the temperature dependence of MR ratio, the red lines are guides to the eyes.

compared with the previously reported temperature dependence of LSMO/Alq_3/Co OSVs, MR decreases much slower for CuPc-based OSVs. Since the only difference between LSMO/Alq_3/Co and LSMO/CuPc/Co OSVs is the organic spacer, the MR temperature dependence can be attributed to the spin relaxation in organic semiconductors.

In order to estimate λ_s in the two types of CuPc films, the MR ratio of the OSV devices was measured with various CuPc thickness at $V = -0.1$ V and $T = 10$ K, as shown in Fig. 4. According to a modified Jullierre model,[1,4] when the MR ratio is well below 100%, the MR ratio exponentially decreases as organic film thickness d increases: $\mathrm{MR} = 2P_{\mathrm{LSMO}}P_{\mathrm{Co}}e^{-d/\lambda_s}$,[11] where P_{LSMO} and P_{Co} are the spin polarizations of LSMO and Co, respectively. From the exponential fitting in Fig. 4, we obtain $\lambda_s = 60$ and 52 nm in the CuPc-1 film and CuPc-2 film, respectively. Although μ of the crystallized CuPc films is ~50 times larger than that of amorphous CuPc, λ_s is almost the same as that of amorphous CuPc. We can use this result to understand the possible dominant spin relaxation mechanism in CuPc.

In organic semiconductors, the charge transport mainly occurs via polaron hopping between localized states, while band-like transport was only observed in a few organic semiconductors. In our experiment, μ is far below the boundary (~1 cm^2/V s) between band transport and hopping transport,[33] suggesting that hopping is the dominating transport mechanism. Therefore, the spin relaxation mechanisms based on the band transport model such as Elliot-Yafet (EY) and the D'yakonov-Perel' (DP) mechanisms is not applicable in our system.[34]

Recently, a spin transport theory in organic materials was proposed that the spin can transport via the exchange coupling between localized carriers rather than hopping.[35] A carrier density n exceeding 10^{17} cm^{-3} is required to establish the exchange coupling between carriers. n in the CuPc films can be estimated from the linear regime of the *J-V* curve [Fig. 2], which is described by $J = ne\mu V/d$. n is estimated to be 10^{15}–10^{16} cm^{-3}, which is one or two order of magnitude smaller than the threshold current density requested for the

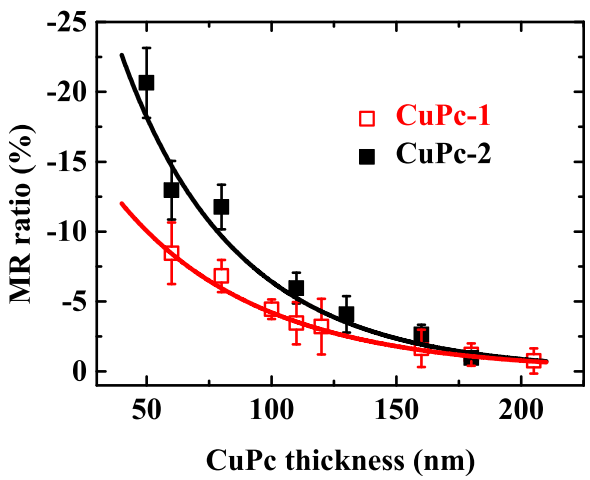

FIG. 4. CuPc thickness dependent MR ratio of LSMO/CuPc/Co OSV devices with CuPc-1 and CuPc-2 as the spacers measured at $T = 10$ K. The error bars are statistical errors due to the averaging of many samples. The solid lines are the exponential fitting.

exchange mechanism, suggesting the inapplicability of the exchange model here, either.

The spin relaxation mechanisms originated from the HFI and SOC were developed for the hopping transport. As for HFI-based mechanism, spins are relaxed by the precession on molecules around the local field, composed of the effective HFI field and the external field, meaning that the spin scattering rate τ_s^{-1} is proportional to the carrier waiting-time τ_w at one molecule: $\tau_s^{-1} \propto \tau_w$.[6] Considering that the Einstein relationship gives $D \propto \mu$ and $\mu \propto 1/\tau_w$, we can get $\lambda_s \propto \sqrt{D\tau_s} \propto \mu$,[6,7] contradictory with our results. On the other hand, as for SOC-based mechanisms, spins flip as they hop from one molecule to another due to the SOC mixing spin up and down states. λ_s is only related with the hopping distance and the SOC strength: $\lambda_s = \bar{R}/4\gamma$, where $\bar{R}$ is the mean hopping distance and the dimensionless parameter γ is determined by the molecule-internal SOC strength. In this model, μ does not have impact on λ_s,[7] consistent with our observations. Hence, our result suggests that the SOC is the dominant spin relaxation source in CuPc and λ_s cannot be enhanced by improving the carrier mobility.

It is worth noting that although λ_s of CuPc-1 film and CuPc-2 film is comparable, the MR ratio of CuPc-1-based OSV is about two times smaller than that of CuPc-2-based OSV. Since the ferromagnetic electrodes and the corresponding spin polarization are the same for devices 1 and 2, we attribute the lower MR ratio of device 1 to the enhanced spin scattering rate at rougher Co/CuPc interface to reduce spin injection efficiency. This interface effect was also observed in other organic materials.[36] The extracted P_{Co} from fitting allows us to estimate the strength of the roughness-induced spin scattering. We obtain $P_{LSMO}P_{Co} = 0.10$ and 0.20 for device 1 and device 2, respectively, from fitting [Fig. 4]. Since the LSMO surface is identical for both devices, P_{LSMO} is assumed to be the same and is ~90% at low temperature.[37] Therefore, P_{Co} is estimated to be ~11% and ~22% for device 1 and device 2, respectively, indicating that the rough interface reduces the effective spin polarization by half. This result suggests that MR ratio does not only depend on the spin diffusion length and hence the method to estimate λ_s relying on MR ratio of a single device is not reliable.[38]

In summary, we compared the magneto-transport properties of LSMO/CuPc/Co OSVs with the CuPc films deposited at different growth conditions. CuPc film grown at high temperature and low growth rate is polycrystalline structure with mobility of 5.78×10^{-3} cm^2/V s. In contrast, CuPc film grown at low temperature and high growth rate is amorphous structure with mobility of 1.11×10^{-4} cm^2/V s. Although the mobility in these two types of CuPc films varies ~50 times, the corresponding spin diffusion length is estimated to be comparable from the MR thickness dependence. This result indicates that the spin relaxation in CuPc is dominated by SOC.

This work was supported by National Basic Research Program of China (2013CB922103), National Nature Science Foundation of China (11222435 and 51471086), and NSF of Jiangsu Province (BK20130054).

[1]Z. H. Xiong, D. Wu, Z. V. Vardeny, and J. Shi, Nature (London) **427**, 821 (2004).
[2]T. D. Nguyen, E. Ehrenfreund, and Z. V. Vardeny, Science **337**, 204 (2012).
[3]M. Prezioso, A. Riminucci, P. Graziosi, I. Bergenti, R. Rakshit, R. Cecchini, A. Vianelli, F. Borgatti, N. Haag, M. Willis, A. J. Drew, W. P. Gillin, and V. A. Dediu, Adv. Mater. **25**, 534 (2013).
[4]T. D. Nguyen, G. Hukic-Markosian, F. Wang, L. Wojcik, X.-G. Li, E. Ehrenfreund, and Z. V. Vardeny, Nat. Mater. **9**, 345 (2010).
[5]A. J. Drew, J. Hoppler, L. Schulz, F. L. Pratt, P. Desai, P. Shakya, T. Kreouzis, W. P. Gillin, A. Suter, N. A. Morley, V. K. Malik, A. Dubroka, K. W. Kim, H. Bouyanfif, F. Bourqui, C. Bernhard, R. Scheuermann, G. J. Nieuwenhuys, T. Prokscha, and E. Morenzoni, Nat. Mater. **8**, 109 (2009).
[6]P. A. Bobbert, W. Wagemans, F. W. A. Van Oost, B. Koopmans, and M. Wohlgenannt, Phys. Rev. Lett. **102**, 156604 (2009).
[7]Z. G. Yu, Phys. Rev. Lett. **106**, 106602 (2011).
[8]N. J. Rolfe, M. Heeney, P. B. Wyatt, A. J. Drew, T. Kreouzis, and W. P. Gillin, Phys. Rev. B **80**, 241201 (2009).
[9]T. D. Nguyen, T. P. Basel, Y.-J. Pu, X. Li, E. Ehrenfreund, and Z. V. Vardeny, Phys. Rev. B **85**, 245437 (2012).
[10]L. Nuccio, M. Willis, L. Schulz, S. Fratini, F. Messina, M. D'Amico, F. L. Pratt, J. S. Lord, I. McKenzie, M. Loth, B. Purushothaman, J. Anthony, M. Heeney, R. M. Wilson, I. Hernández, M. Cannas, K. Sedlak, T. Kreouzis, W. P. Gillin, C. Bernhard, and A. J. Drew, Phys. Rev. Lett. **110**, 216602 (2013).
[11]B. B. Chen, S. Wang, S. W. Jiang, Z. G. Yu, X. G. Wan, H. F. Ding, and D. Wu, New J. Phys. **17**, 013004 (2015).
[12]G. Szulczewski, S. Sanvito, and M. Coey, Nat. Mater. **8**, 693 (2009).
[13]V. A. Dediu, L. E. Hueso, I. Bergenti, and C. Taliani, Nat. Mater. **8**, 707 (2009).
[14]J. H. Shim, K. V. Raman, Y. J. Park, T. S. Santos, G. X. Miao, B. Satpati, and J. S. Moodera, Phys. Rev. Lett. **100**, 226603 (2008).
[15]Z. G. Yu, F. Ding, and H. Wang, Phys. Rev. B **87**, 205446 (2013).
[16]Z. N. Bao, A. J. Lovinger, and A. Dodabalapur, Appl. Phys. Lett. **69**, 3066 (1996).
[17]S. Wang, Y. J. Shi, L. Lin, B. B. Chen, F. J. Yue, J. Du, H. F. Ding, F. M. Zhang, and D. Wu, Synth. Met. **161**, 1738 (2011).
[18]M. Della Pirriera, J. Puigdollers, C. Voz, M. Stella, J. Bertomeu, and R. Alcubilla, J. Phys. D: Appl. Phys. **42**, 145102 (2009).
[19]R. R. Lunt, J. B. Benziger, and S. R. Forrest, Appl. Phys. Lett. **90**, 181932 (2007).
[20]M. Minohara, I. Ohkubo, H. Kumigashira, and M. Oshima, Appl. Phys. Lett. **90**, 132123 (2007).
[21]Y. Q. Zhan, M. P. De Jong, F. H. Li, V. Dediu, M. Fahlman, and W. R. Salaneck, Phys. Rev. B **78**, 045208 (2008).
[22]A. K. Mahapatro and S. Ghosh, J. Appl. Phys. **101**, 034318 (2007).
[23]F. J. Yue, Y. J. Shi, B. B. Chen, H. F. Ding, F. M. Zhang, and D. Wu, Appl. Phys. Lett. **101**, 022416 (2012).
[24]A. K. Mahapatro and S. Ghosh, Appl. Phys. Lett. **80**, 4840 (2002).
[25]Z. Chiguvare and V. Dyakonov, Phys. Rev. B **70**, 235207 (2004).
[26]K. R. Choudhury, J. Yoon, and F. So, Adv. Mater. **20**, 1456 (2008).
[27]R. D. Gould, J. Phys. D: Appl. Phys. **19**, 1785 (1986).
[28]D. R. Lide, *CRC Handbook of Chemistry and Physics*, 90th ed. (CRC, Boca Raton, 2010).
[29]P. Sullivan, T. S. Jones, A. J. Ferguson, and S. Heutz, Appl. Phys. Lett. **91**, 233114 (2007).
[30]F. J. Wang, Z. H. Xiong, D. Wu, J. Shi, and Z. V. Vardeny, Synth. Met. **155**, 172 (2005).
[31]F. J. Wang, C. G. Yang, Z. V. Vardeny, and X. G. Li, Phys. Rev. B **75**, 245324 (2007).
[32]V. Dediu, L. E. Hueso, I. Bergenti, A. Riminucci, F. Borgatti, P. Graziosi, C. Newby, F. Casoli, M. P. De Jong, C. Taliani, and Y. Zhan, Phys. Rev. B **78**, 115203 (2008).
[33]C. D. Dimitrakopoulos and P. R. L. Malenfant, Adv. Mater. **14**, 99 (2002).
[34]I. Bergenti, V. Dediu, M. Prezioso, and A. Riminucci, Philos. Trans. R. Soc., A **369**, 3054 (2011).
[35]Z. G. Yu, Phys. Rev. Lett. **111**, 016601 (2013).
[36]Y. Liu, S. M. Watson, T. Lee, J. M. Gorham, H. E. Katz, J. A. Borchers, H. D. Fairbrother, and D. H. Reich, Phys. Rev. B **79**, 075312 (2009).
[37]B. Nadgorny, I. I. Mazin, M. Osofsky, R. J. Soulen, Jr., P. Broussard, R. M. Stroud, D. J. Singh, V. G. Harris, A. Arsenov, and Y. Mukovskii, Phys. Rev. B **63**, 184433 (2001).
[38]K. M. Alam, S. C. Bodepudi, R. Starko-Bowes, and S. Pramanik, Appl. Phys. Lett. **101**, 192403 (2012).